Engineering soliton nonlinearities: from local to strongly nonlocal

Yaroslav V. Kartashov,* Victor A. Vysloukh, and Lluis Torner

ICFO–Institut de Ciencies Fotoniques and Universitat Politecnica de Catalunya, Mediterranean Technology Park, 08860 Castelldefels, Barcelona, Spain

**Corresponding author: Yaroslav.Kartashov@icfo.es*

Received January 30, 2009; revised March 18, 2009; accepted April 15, 2009; posted April 20, 2009 (Doc. ID 106999); published May 11, 2009

We put forward what we believe to be a novel strategy to achieve synthetic nonlinearities where local and nonlocal contributions compete on a similar footing, thus yielding intermediate tunable responses ranging from local to strongly nonlocal. The setting addressed is a semiconductor material with both Kerr and thermal nonlinearities illuminated by a pulse train with suitable pulse width and repetition rate.

OCIS codes: 190.0190, 190.6135.

The type of nonlinear response of a given material determines the phenomena exhibited by an intense beam propagating in it. An example is provided by nonlocal versus local nonlinearities, a difference that may lead to drastic differences in light evolution. For example, in contrast to uniform media with local cubic nonlinearities where multidimensional and higher-order solitons are unstable, nonlocal nonlinearities arrest collapse [1], change the character of soliton interactions [2,3] making possible the existence of bound soliton states [4–8], and stabilize vortex solitons [9–11]. Tuning the nonlinear response from predominantly local to predominantly nonlocal is possible in suitable materials [12], while the competition of nonlinearities with different nonlocality degrees was considered in phenomenological models [13,14], dipolar Bose–Einstein condensates [15,16], and in Salerno models [17]. This is a potentially far-reaching program because access to intermediate nonlinear responses may open a new door to the new phenomena not possible in the limiting cases.

In this Letter, we develop what we believe to be a new strategy to explore the intermediate local–nonlocal response. We consider a semiconductor material, such as AlGaAs [18–20], where the contribution to the refractive index $\delta n \sim 10^{-4}$ owing to the Kerr effect requires peak intensities $I \sim \mathrm{GW/cm^2}$. A similar refractive index change might be achieved owing to thermal nonlinearity by heating with a cw beam carrying $I \sim 100\ \mathrm{W/cm^2}$ focused down to a spot size of $\sim 10\ \mu$m. Note that soliton experiments in AlGaAs are regularly conducted with high peak-power pulsed light [19,20], but thermal nonlinearity is weak because such pulses carry a very small total energy. By tuning the pulse duration and repetition rate, we study scenarios where the strength of local Kerr and nonlocal thermal nonlinearities becomes comparable thus yielding an intermediate local–nonlocal nonlinearity. Such synthetic response supports multipole solitons that are stable for any number of poles, a phenomenon that does not occur in either the local or nonlocal limiting cases.

We address the propagation of a light beam along the ξ axis of planar waveguide of width L, whose left and right edges at $\eta = \pm L/2$ are thermostabilized at the temperature T_0. The beam is slightly absorbed upon propagation, thus acting as a heat source that generates an inhomogeneous temperature distribution. Thus, the light beam experiences both the Kerr and thermal nonlinearities. We assume pulsed illumination, a key ingredient to control the relative strength of the Kerr and thermal nonlinearities. The light propagation is described by the equation for the field amplitude q coupled to the thermal conductivity equation for the temperature distribution θ,

$$i\frac{\partial q}{\partial \xi} = -\frac{1}{2}\frac{\partial^2 q}{\partial \eta^2} - |q|^2 q - \gamma\theta q,$$

$$\frac{\partial \theta}{\partial \tau} - \frac{\partial^2 \theta}{\partial \eta^2} = \phi(\tau)|q|^2. \qquad (1)$$

Here $\xi = z/k_0 x_0^2$ is the propagation distance normalized to the diffraction length $k_0 x_0^2$; $\eta = x/x_0$ is the normalized transverse coordinate; $q = (k_0 x_0^2 \omega n_2/c)^{1/2} E$ is the field amplitude; n_2 is the Kerr nonlinearity coefficient; $\tau = t\kappa/x_0^2$ is the normalized time; κ is the thermodiffusion coefficient; $\theta = (\rho C_p \kappa \omega n_2 k_0/\alpha c)(T - T_0)$ is the normalized temperature and $\theta|_{\eta=\pm L/2} = 0$; ρ is the density; C_p is the specific heat capacity; α is the absorption coefficient; $\gamma = \alpha\beta x_0^2/n_2 \rho C_p \kappa$; and β is the thermo-optic coefficient. The function $\phi(\tau)$ describes a train of Gaussian pulses $\exp(-\tau^2/\tau_{\mathrm{dur}}^2)$ with width τ_{dur} and repetition period $\tau_{\mathrm{rep}} \gg \tau_{\mathrm{dur}}$. For AlGaAs under typical conditions one has $\alpha \approx 0.2\ \mathrm{cm^{-1}}$, $n_2 \approx 1.5 \times 10^{-13}\ \mathrm{cm^2/W}$ at $\lambda = 1.55\ \mu$m, $\beta \approx 2.7 \times 10^{-4}\ \mathrm{K^{-1}}$, $\rho = 5\ \mathrm{g/cm^3}$, $C_p \approx 0.33\ \mathrm{J/gK}$, and $\kappa \approx 0.1\ \mathrm{cm^2/s}$. Thus, $x_0 = 10\ \mu$m yields $x_0^2/\kappa \approx 10^{-5}$ s, $\alpha c/\rho C_p \kappa \omega n_2 k_0 \approx 1440$ K, and $\gamma = 21.6$. For these parameters $\gamma\theta \approx 0.45$ corresponds to $T - T_0 \sim 30$ K. We set $L = 20$.

Figure 1 shows the spatiotemporal temperature distribution in a sample heated by a pulse train. When each pulse arrives it raises the temperature in the region of highest intensity. The peak intensity of each pulse is sufficiently high, so that around the

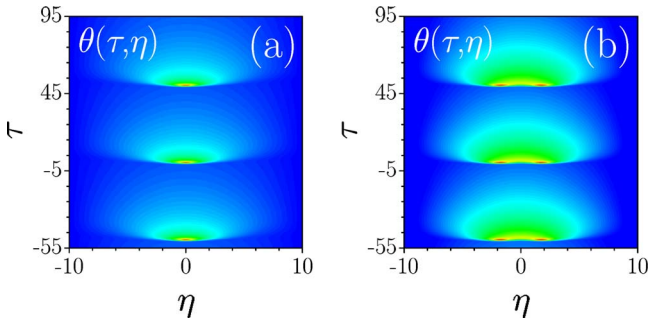

Fig. 1. (Color online) Typical spatiotemporal temperature distributions upon heating of the sample with pulse sequence when transverse intensity distribution features (a) one or (b) two humps. In both cases $\tau_{rep}=50$ and $\tau_{dur}=0.5$.

pulse peak the Kerr nonlinearity is significant. In turn, the temperature distribution is dictated by the absorbed energy. When τ_{dur} is small the increase in θ generated by each pulse is small. After each pulse θ decays, so that for $\tau_{rep}\to\infty$ the temperature between subsequent pulses decreases to negligible values. However, as τ_{dur} increases and τ_{rep} decreases the temperature does not decrease between pulses, and a significant thermal lens builds up inside the sample that impacts beam evolution with a strength that may be comparable to that caused by the Kerr nonlinearity. Thus, by varying the parameters of the pulse train one may engineer the overall response of the material from fully local to strongly nonlocal.

At first approximation one may use in the first equation of Eq. (1) the temperature profile $\theta(\eta,\tau=0)$ taken at the pulse peak $\tau=0$. This is justified as long as the on-axis temperature variation $\theta_d=(\theta_{max}-\theta_{min})|_{\eta=0}$ is not too large in comparison to $\theta_0=\theta|_{\eta=\tau=0}$. Thus, $\theta(\eta,\tau=0)$ serves as an external transverse potential in Eq. (1), whose shape depends on the spatial intensity distribution $|q(\eta,\xi)|^2$ and the pulse sequence $\phi(\tau)$. This allows one to obtain spatial soliton solutions of Eq. (1) in the form $q=w(\eta)\exp(ib\xi)$. The temporal intensity distribution is frozen and given by $\phi(\tau)I=\phi(\tau)w^2$.

Figure 2 shows typical soliton shapes (note that the beam is only trapped in space) and corresponding temperature distributions. The presence of nonlocal thermal nonlinearities affords the existence of multipole solitons, which cannot exist in local Kerr materials. The simplest dipole soliton is shown in Figs. 2(c) and 2(d). With increasing peak intensity, the on-axis temperature θ_0 and its variation θ_d grow [Figs. 2(a) and 2(c)]. The temperature grows in a noticeable way only in the region where the pulse intensity is significant and slowly decreases between pulses. One can see the appearance of local maxima (whose positions overlap with intensity maxima) on top of the otherwise smooth and broad spatial temperature distributions [Figs. 2(b) and 2(d)], which is in contrast to spatial temperature distributions in the steady-state case, where θ always increases monotonically toward the beam center, even for multipoles. The local maxima become more pronounced as the temporal temperature variation θ_d increases, i.e., as b grows. In the case of multipoles the separation between intensity maxima decreases with increasing peak intensity.

The energy flow of the exact fundamental soliton, defined as $U=\int_{-\infty}^{\infty}|q|^2 d\eta$, increases monotonically with b [Fig. 3(a)]. At fixed b the energy flow attains its maximum value in the limit $\tau_{dur}\to 0$ when the thermal nonlinearity vanishes and $w\to(2b)^{1/2}\,\mathrm{sech}[(2b)^{1/2}\eta]$. With increasing τ_{dur} the focusing thermal contribution becomes more pronounced and causes a decrease in the peak intensity (hence U) necessary for stationary propagation. Decreasing τ_{rep} also results in a decrease in U at a fixed b. At fixed b and τ_{dur} the on-axis temperature θ_0 is a monotonically decreasing function of τ_{rep}, while the on-axis temperature variation θ_d first increases and then asymptotically approaches a constant value as $\tau_{rep}\to\infty$ [Fig. 3(b)]. When τ_{rep} decreases θ does not decrease significantly between subsequent pulses that results in the increase in the stationary part of the temperature distribution as well as in an increase in θ_0. This makes the thermal lens stronger so that the soliton amplitude at fixed b decreases and each pulse carries a smaller energy, resulting in a lower temperature variation θ_d upon the passing of the single pulse. In this regime, the thermal response dominates over the Kerr effect and it is reminiscent of the thermal response in the steady state.

In the other limit, when $\tau_{rep}\to\infty$, the temperature relaxes almost completely between subsequent pulses, the stationary part of the temperature dimin-

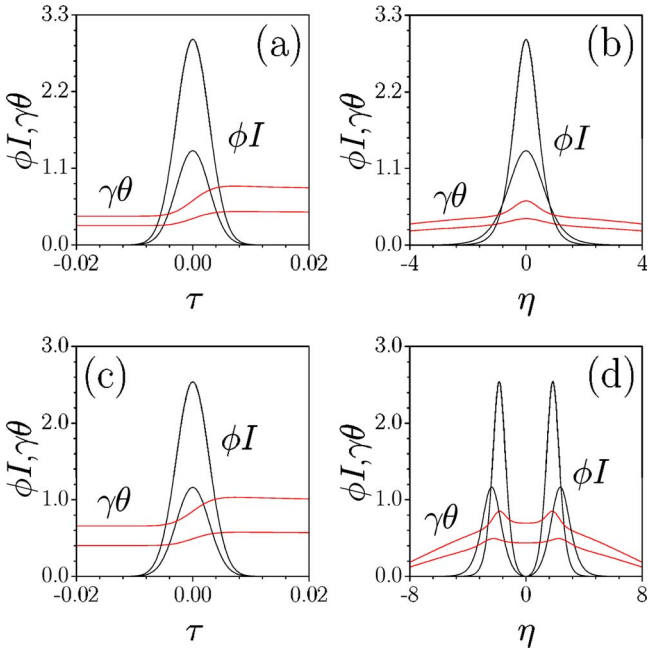

Fig. 2. (Color online) (a),(c) Temporal and (b),(d) spatial distributions at $\tau=0$ of intensity ϕI (black curves) and temperature $\gamma\theta$ [gray (red online) curves] for fundamental (top) and dipole (bottom) solitons at $\tau_{rep}=5$ and $\tau_{dur}=0.004$. Upper curves in each panel correspond to $b=2$; lower curves correspond to $b=1$. For fundamental solitons temporal distributions are shown at $\eta=0$, while for dipoles they are shown at the point corresponding to the intensity maximum.

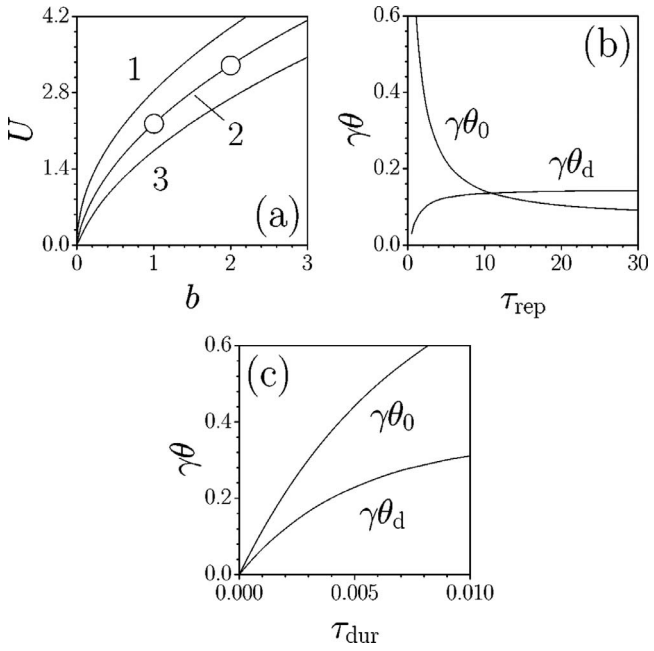

Fig. 3. (a) U versus b for the fundamental soliton at $\tau_{rep}=5$ for (a) $\tau_{dur}\to 0$, (2) $\tau_{dur}=0.004$, and (3) $\tau_{dur}=0.009$. Circles correspond to the solitons in Figs. 2(a) and 2(b). Temperature $\gamma\theta_0$ at $\eta=\tau=0$ and maximal temperature difference $\gamma\theta_d$ at $\eta=0$ versus (b) τ_{rep} at $\tau_{dur}=0.002$ and versus (c) τ_{dur} at $\tau_{rep}=5$. In (b) and (c) $b=1$.

ishes, and θ_d is determined by the energy carried by each pulse. In this case the soliton amplitude and θ_d asymptotically approach constant values. Notice that when one keeps fixed U instead of b, the θ_d value does not change with τ_{rep}, while θ_0 decreases with τ_{rep}. Increasing τ_{dur} at a fixed b and τ_{rep} results in a monotonic growth of θ_0 and θ_d [Fig. 3(c)]. The limit $\tau_{dur}\to 0$ corresponds to a negligible heating of the material and domination of the Kerr nonlinearity. These results clearly show the possibility to control the relative weights of the Kerr and thermal nonlinearities by varying τ_{dur} and τ_{rep}.

An example of the new phenomena made possible by the competing local–nonlocal nonlinearities is in order. On physical grounds, the specific spatial temperature distribution featuring local maxima around the soliton peaks may affect profoundly the soliton stability. While the stability of fundamental solitons in this system is not surprising, we found that multipoles can be stable too, *for an unlimited number of poles*. This is in clear contrast to both limits of the local Kerr nonlinearity, where multipoles do not even exist, and of the purely nonlocal steady-state thermal nonlinearity, where the number of stable poles was found to be limited to a maximal number [5]. Examples of the stable propagation of two- and five-hump solitons (perturbed by the addition of initial noise) are shown in Fig. 4 for parameter values where the Kerr and the thermal nonlinear contributions amount to comparable values. We tested multipoles containing up to ten poles and found that all of them appear to be stable.

We thus conclude by stressing that the scheme put forward here affords the possibility to realize intermediate nonlinear responses where local and nonlocal components compete on similar footing, generating new phenomena not accessible in purely local or nonlocal media.

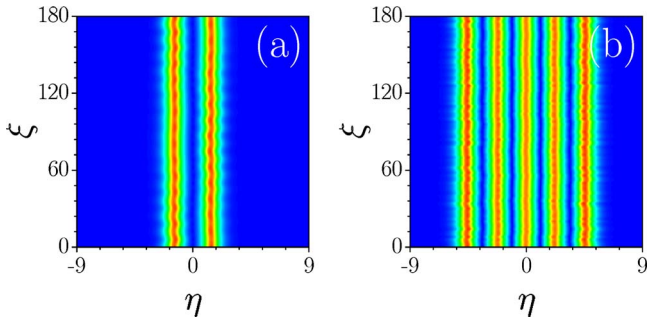

Fig. 4. (Color online) Stable propagation of perturbed (a) dipole and (b) five-hump solitons with $b=4$, $\tau_{rep}=5$, and $\tau_{dur}=0.004$.

References

1. W. Krolikowski, O. Bang, N. I. Nikolov, D. Neshev, J. Wyller, J. J. Rasmussen, and D. Edmundson, J. Opt. B **6**, S288 (2004).
2. M. Peccianti, K. A. Brzdakiewicz, and G. Assanto, Opt. Lett. **27**, 1460 (2002).
3. C. Rotschild, B. Alfassi, O. Cohen, and M. Segev, Nat. Phys. **2**, 769 (2006).
4. X. Hutsebaut, C. Cambournac, M. Haelterman, A. Adamski, and K. Neyts, Opt. Commun. **233**, 211 (2004).
5. Z. Xu, Y. V. Kartashov, and L. Torner, Opt. Lett. **30**, 3171 (2005).
6. S. Lopez-Aguayo, A. S. Desyatnikov, Y. S. Kivshar, S. Skupin, W. Krolikowski, and O. Bang, Opt. Lett. **31**, 1100 (2006).
7. Y. V. Kartashov, L. Torner, V. A. Vysloukh, and D. Mihalache, Opt. Lett. **31**, 1483 (2006).
8. C. Rotschild, M. Segev, Z. Xu, Y. V. Kartashov, L. Torner, and O. Cohen, Opt. Lett. **31**, 3312 (2006).
9. D. Briedis, D. Petersen, D. Edmundson, W. Krolikowski, and O. Bang, Opt. Express **13**, 435 (2005).
10. A. I. Yakimenko, Y. A. Zaliznyak, and Y. Kivshar, Phys. Rev. E **71**, 065603(R) (2005).
11. C. Rotschild, O. Cohen, O. Manela, M. Segev, and T. Carmon, Phys. Rev. Lett. **95**, 213904 (2005).
12. M. Peccianti, C. Conti, and G. Assanto, Opt. Lett. **30**, 415 (2005).
13. D. Mihalache, D. Mazilu, F. Lederer, L.-C. Crasovan, Y. V. Kartashov, L. Torner, and B. A. Malomed, Phys. Rev. E **74**, 066614 (2006).
14. Y. V. Kartashov, V. A. Vysloukh, and L. Torner, Phys. Rev. A **79**, 013803 (2009).
15. P. Pedri and L. Santos, Phys. Rev. Lett. **95**, 200404 (2005).
16. I. Tikhonenkov, B. A. Malomed, and A. Vardi, Phys. Rev. A **78**, 043614 (2008).
17. J. Gomez-Gardenes, B. A. Malomed, L. M. Floria, and A. R. Bishop, Phys. Rev. E **73**, 036608 (2006).
18. P. S. Dobal, H. D. Bist, S. K. Mehta, and R. K. Jain, Appl. Phys. Lett. **65**, 2469 (1994).
19. J. S. Aitchison, D. C. Hutchings, J. U. Kang, G. I. Stegeman, and A. Villeneuve, IEEE J. Quantum Electron. **33**, 341 (1997).
20. J. S. Aitchison, K. Al-Hemyari, C. N. Ironside, R. S. Grant, and W. Sibbett, Electron. Lett. **28**, 1879 (1992).